



Research papers

Using stable isotopes to assess surface water source dynamics and hydrological connectivity in a high-latitude wetland and permafrost influenced landscape



P. Ala-aho^{a,*}, C. Soulsby^a, O.S. Pokrovsky^{b,c}, S.N. Kirpotin^d, J. Karlsson^e, S. Serikova^e, S.N. Vorobyev^d, R.M. Manasyrov^d, S. Loiko^d, D. Tetzlaff^a

^a Northern Rivers Institute, School of Geosciences, University of Aberdeen, UK

^b GET UMR 5563 CNRS, University of Toulouse, France

^c N. Laverov Federal Center for Integrated Arctic Research, Russian Academy of Science, Russia

^d BIO-GEO-CLIM Laboratory, Tomsk State University, Russia

^e Department of Ecology and Environmental Science, Umeå University, Sweden

ARTICLE INFO

Article history:

Received 19 May 2017

Received in revised form 2 October 2017

Accepted 13 November 2017

Available online 14 November 2017

This manuscript was handled by T. McVicar, Editor-in-Chief, with the assistance of Huade Guan, Associate Editor

Keywords:

Stable water isotopes

Hydrological connectivity

Runoff generation

Snowmelt

Low-relief

ABSTRACT

Climate change is expected to alter hydrological and biogeochemical processes in high-latitude inland waters. A critical question for understanding contemporary and future responses to environmental change is how the spatio-temporal dynamics of runoff generation processes will be affected. We sampled stable water isotopes in soils, lakes and rivers on an unprecedented spatio-temporal scale along a 1700 km transect over three years in the Western Siberia Lowlands. Our findings suggest that snowmelt mixes with, and displaces, large volumes of water stored in the organic soils and lakes to generate runoff during the thaw season. Furthermore, we saw a persistent hydrological connection between water bodies and the landscape across permafrost regions. Our findings help to bridge the understanding between small and large scale hydrological studies in high-latitude systems. These isotope data provide a means to conceptualise hydrological connectivity in permafrost and wetland influenced regions, which is needed for an improved understanding of future biogeochemical changes.

© 2017 The Authors. Published by Elsevier B.V. This is an open access article under the CC BY license (<http://creativecommons.org/licenses/by/4.0/>).

1. Introduction

High-latitude regions are experiencing alarming hydrological changes as a consequence of global climate change (IPCC, 2014; Tetzlaff et al., 2013; Walvoord and Kurylyk, 2016; White et al., 2007). The future climate is expected to result in a multitude of hydrologically important changes in precipitation patterns and frequencies (Lenderink and Meijgaard, 2008; Bintanja and Selten, 2014), water vapour pressure (Willett et al., 2008), and wind speed (McVicar et al., 2012). In high-latitude regions air temperature is a crucial control for the cryogenic processes that play a key role in their energy and water balances (Woo et al., 2008; Wild, 2009). Recent literature reports accelerating rates of permafrost thaw, which is expected to have cascading effects on the high-latitude environment, river flow regimes and associated biogeochemical

interactions (Frey and McClelland, 2009; Giesler et al., 2014; Lyon et al., 2009). Of particular importance is the amplified release of organic carbon due to permafrost thaw (Frey and Smith, 2005; Kuhry et al., 2010; Lessels et al., 2015; O'Donnell et al., 2012). However, the hydrological connections that determine carbon mobilization and fluxes in high-latitude watersheds remain inadequately understood (Yi et al., 2012; Zakharova et al., 2014).

The hydrology of high-latitude areas differs from temperate climates due to the strong influence of permafrost, extensive lake and wetland distribution and the transmissive properties of the dominant organic soils (Bowling et al., 2003; Carey and Quinton, 2004; Quinton and Marsh, 1999; Woo et al., 2008; Zakharova et al., 2014). Thawing permafrost is altering the hydrological regime and overall landscape structure, by either increasing the number of lakes in continuous permafrost regions by thermokarst development, or decreasing lake number and surface area by accelerated drainage of thermokarst lakes in discontinuous permafrost terrain (Smith et al., 2007b; Smith et al., 2005). Deepening the active layer and associated changes in lake and wetland distribution alter

* Corresponding author at: School of Geosciences, University of Aberdeen, Elphinstone Road, Aberdeen AB24 3UF, UK.

E-mail address: perti.ala-aho@abdn.ac.uk (P. Ala-aho).

landscape-scale hydrological connectivity (Quinton et al., 2011; Smith et al., 2007b; Zakharova et al., 2014). This is expected to result in deeper hydrological flow paths, thus increasing water travel times and hydrological connectivity in the north (Frampton and Destouni, 2015; Karlsson et al., 2012). It has been suggested that these changes have resulted in an increased discharge of major rivers draining Pan-Arctic watersheds (Peterson et al., 2002; Smith et al., 2007a).

Stable water isotopes of hydrogen ($\delta^2\text{H}$) and oxygen ($\delta^{18}\text{O}$) provide a useful and increasingly applied tool for integrating hydrological process information across various scales (McDonnell and Beven, 2014). Existing isotope hydrology studies in high-latitude areas have been mostly conducted on two contrasting scales. One line of isotope work has looked into large scale hydrological responses at the outlets of major Pan-Arctic watersheds ($\sim 10^5$ – 10^6 km²), leading to improved understanding of the main river source water that drain into the Arctic Ocean (Cooper et al., 2008; Welp et al., 2005; Yi et al., 2012). At the other end of the spectrum, isotope studies at the hillslope and headwater catchment scale (typically 1–100 km²) have substantially increased understanding of detailed hydrological processes contributing to runoff generation for high-latitude (including permafrost influenced) catchments (Carey and Quinton, 2004; Hayashi et al., 2004; Song et al., 2017; Streletskiy et al., 2015; Tetzlaff et al., 2015b; Throckmorton et al., 2016).

There has been some stable water isotope work at the 'intermediate' scale (10^2 – 10^5 km²), between the small and the large scale studies, to determine evaporation signals and rates in high-latitude lakes (Gibson, 2001; Narancic et al., 2017) and studying footprints of climatic forcing on river isotope composition (Lachniet et al., 2016). This important work in high-latitude environments is from landscapes where topography exerts a major control on hydrology. Water sources, flow paths and drainage structures in low-relief watersheds strongly affected by permafrost or lakes/wetlands are much less extensively researched (Zakharova et al., 2009; Zakharova et al., 2011), particularly at scales that would address intermediate scales and bridge the gap from small experimental catchments to regional and continental scale watersheds (Jasechko et al., 2017; Woo et al., 2008; Yi et al., 2012). A major knowledge gap remains as to how small scale runoff generation processes aggregate into a watershed response in high-latitude areas.

We seek to address this research gap. The specific objectives of our work are: (i) to map the spatio-temporal variability of stable water isotope composition in rivers, soils, lakes, and snow over multiple seasons and years along a 11° latitudinal gradient from the boreal permafrost-free south to the northern Arctic permafrost-dominated environments in Western Siberia; (ii) understand temporal changes in water sources of the river Ob by collecting a high resolution river water isotope time series; and (iii) based on the isotopic signatures, we formulate an improved conceptual understanding of the internal drainage structure of this vast wetland and permafrost influenced high-latitude region, that links small scale process understanding to regional watershed response.

2. Materials and methods

2.1. Study transect in the Western Siberia Lowlands

Our study area encompasses a 1700 km long transect in the Western Siberia Lowlands (WSL) encompassing three major high-latitude watersheds: the Ob, Pur and Taz with total watershed areas of 2,972,000, 112,000, and 150,000 km², respectively. The transect (Fig. 1) runs primarily northwest in the Ob watershed

between 56 and 62°N and turns northeast crossing the Pur watershed between 63 and 66.3°N and the Taz watershed (66.9–67.5°N), spanning in total $\sim 11^\circ$ latitude (~ 1200 km from south to north).

Except for the northern part of the Pur and the Taz, the WSL has a moderate continental climate with marked seasonal variability between short summers and long cold winters. The mean annual temperature ranges from -0.5°C in the southern parts of the transect, gradually decreasing with latitude down to -9.5°C in the north. Annual precipitation is lowest in the southern areas with 550 mm, increases to 650–700 mm around 63°N and reduces to 600 mm at the northern parts. Rivers sampled in the Ob watershed ($<63^\circ\text{N}$) are on permafrost-free areas in the southern region (approx. $<60^\circ\text{N}$) and on isolated (60 – 62°N) and sporadic and discontinuous (62 – 63°N) permafrost in the north (Brown et al., 2002). Sampled rivers in the Pur watershed ($>63^\circ\text{N}$) all run on sporadic and discontinuous permafrost, and samples taken from the Taz ($>67^\circ\text{N}$) watershed are on continuous permafrost. Annual runoff increases northward with 160–220 mm a⁻¹ in the southern permafrost-free zone to 280–320 mm a⁻¹ in the permafrost affected northern areas.

The geology of the WSL consist of sedimentary rocks, dominated by sandstones and shales (Ulmishek, 2003) overlain by Quaternary aeolian and fluvial sand, silt and clay deposits ranging from a few meters to 200–250 m in thickness (Pokrovsky et al., 2015). Because of the cool air temperatures, flat relief, and waterlogged conditions, the area is dominated by organic peat soils with thickness between 1 and 3 m mantling the mineral sub-soils (Frey et al., 2007). Peatlands in the WSL are dominated by ombrogenous bogs (hydrologically sourced by precipitation), fens (sourced by precipitation and lateral surface and subsurface groundwater flow) and lakes (Kirpotin et al., 2009). In the permafrost zone, lakes typically form in response to thermal erosion and permafrost thaw (thermokarst), whereas in the permafrost-free areas peat erosion is the key process of lake formation. Wetland and lake cover in the WSL can vary from 20 to 80 percent over the year, depending on the seasonal hydrological conditions (Zakharova et al., 2014). Previous work in the WSL has quantitatively shown their importance in dynamically modulating streamflow response by storing snowmelt and rainfall, but more detailed process understanding of their influence on runoff generation is needed (Zakharova et al., 2009; Zakharova et al., 2011).

The WSL offer a natural laboratory to study large scale lowland hydrology in an area with a spectrum of soil frost and permafrost conditions, relatively homogenous geology with sedimentary basement rock, minimal orographic influences and uniform annual precipitation (Pokrovsky et al., 2015; Zakharova et al., 2014). Our hydrological understanding of the WSL needs to be improved because of its profound importance for global carbon, nutrient and fresh water delivery to the Arctic Ocean (Frey and Smith, 2005; Pokrovsky et al., 2015; Smith and Alsdorf, 1998). Furthermore, among high-latitude areas, the WSL are especially vulnerable to climate change as much of the area resides in the discontinuous permafrost zone where small increases in temperature can lead to drastic changes in permafrost conditions (Kirpotin et al., 2009; Romanovsky et al., 2010).

2.2. Stable water isotope sampling design and protocols

River sampling was focused on the main stem and tributaries ($n = 59$) of the Ob, Taz and Pur rivers along the study transect (Fig. 1). Catchment areas of the sampling locations varied between 10 and 7.7 10^5 km² (median 270.8 km²). Rivers were primarily sampled between 2014 and 2015 with three major seasonal campaigns in both years: firstly, targeting baseflow during the winter snow-covered period in February–March, secondly, sampling the snowmelt period between April–May, and the final one targeting

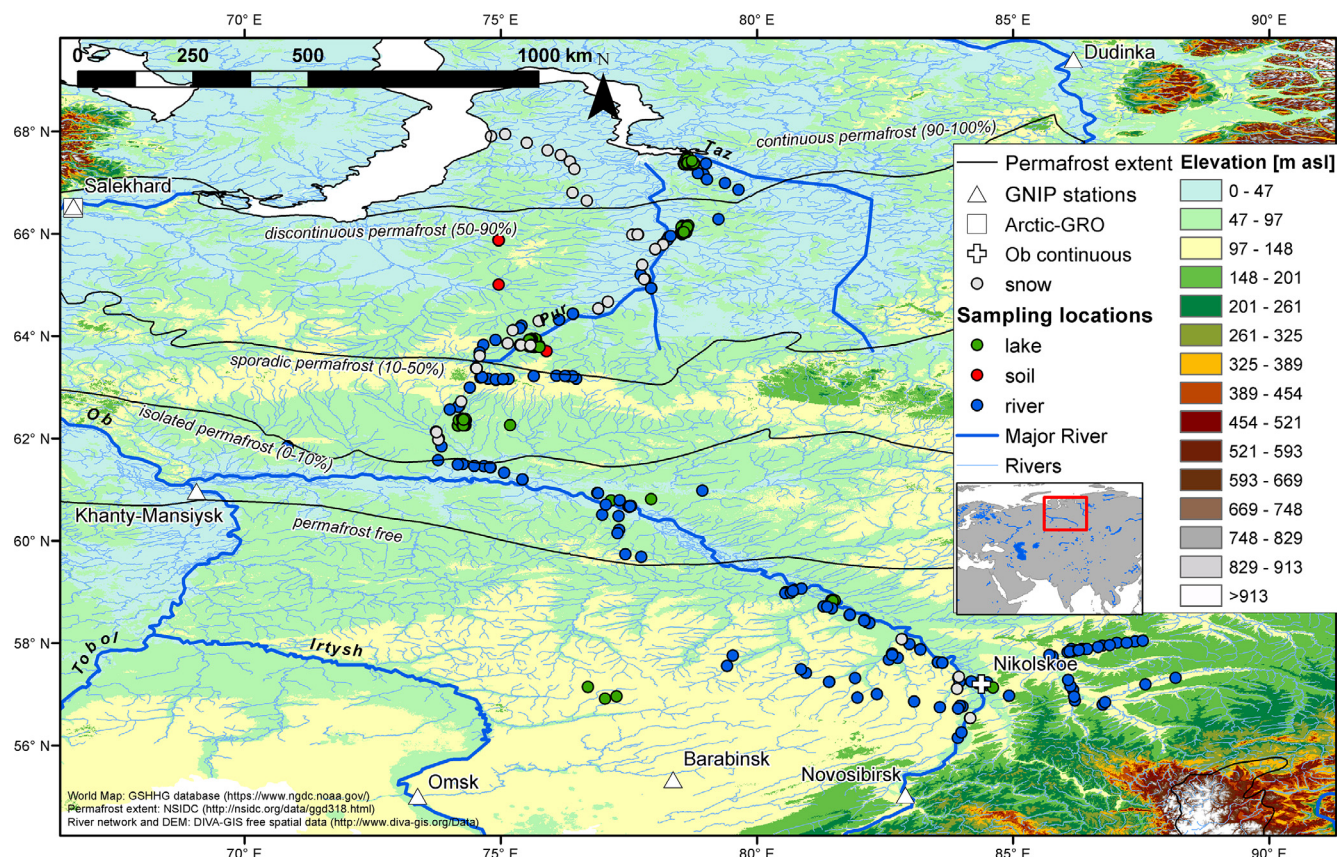


Fig. 1. Overview of the study area showing isotope sampling locations, GNIP precipitation stations, Arctic-GRO monitoring location in Salekhard, and location of high frequency isotope sampling in the Ob at Nikolskoe. Permafrost extent is delineated according to Brown et al. (2002). Supplementary material S1 singles out sampled locations for different river sampling campaigns, lakes and soils with less overlap.

the summer flows in July–August. Because of the large sampling area, logistical challenges prevented us from sampling all tributaries in all campaigns. The sampled locations for each campaign are shown in the Supplementary material (Fig. S2). Some additional river samples from different tributaries were collected throughout the intensive monitoring, and in the summer of 2016. Sampling was achieved by grab sample collection from the middle of the river channel if possible from a bridge, or from the river banks, from the depth of 0.5 m within the actively flowing river (never stagnant water).

Lake sampling was primarily focused in the open water season of 2016. The majority of the samples were collected from four lake clusters representing different permafrost zones (Fig. S2): Kogalym (62.3 N), Kahnymey (63.8 N), Urengoy (66.0 N) and Tazovky (67.4 N) with the first campaign occurred immediately after snowmelt when the lakes become accessible in May–June, second in midsummer in August and the final sampling before freeze-up in September–October (Fig. S2).

Lake water samples were taken from a boat in the middle of each lake at a depth of 0.5 m. Thermokarst lakes of WSL are extremely shallow (1.0 ± 0.5 m depth, (Polishchuk et al., 2017)), and therefore the depth of sampling at the small lakes (<1000 m² area) was 0.25 m. If water had excess organic matter, samples were filtered immediately on site using sterile plastic syringes through single-use pre-washed acetate cellulose filter units. The first 2 ml of filtrate were discarded.

The soil solutions were sampled in the summer of 2015 primarily from four areas coinciding with the lake sampling in Kogalym, Kahnymey, and Tazovky and with a more western location at the latitude of Urengoy (Fig. S2). The sampling was done with ceramic

cup suction lysimeters, and from variable depths in the active layer, between 20 and 50 cm, which was typically 10 cm above the permafrost table. Soil samples were filtered in the field using Sartorius 0.45 μ m filters and syringes. Details of soil solution sampling are given in Raudina et al. (2017).

In addition to our spatially distributed sampling, we performed local high frequency sampling of the Ob mid-reaches at Kaibasovo, 16 km upstream of the Nikolskoe river stage gauging station (Fig. 1). The sampling interval was initially monthly, starting in Jan 2015, then every two days between 30 Oct 2015–24 Apr 2016, and every day for snowmelt period 24 April – 31 May 2016. Sampling was conducted as grab sampling 2 m offshore in an area of free river flow.

All samples were collected into 3.5 ml glass vials and stored in the dark at 4–6 °C until analysis. Samples were analysed at the University of Aberdeen using a Los Gatos DLT-100 laser isotope analyser with instrument precision $\pm 0.4\%$ for $\delta^2\text{H}$ and $\pm 0.1\%$ for $\delta^{18}\text{O}$. Isotope ratios are reported in the δ -notation using the Vienna Standard Mean Ocean Water standards (Coplen, 1994).

2.3. Secondary data sources

To further improve our understanding of the isotope hydrology of the WSL using hydrometeorological data to support our analysis, we utilised data from the following additional sources. Stable water isotopes in precipitation were downloaded from the GNIP database (IAEA/WMO, 2017; Kurita et al., 2004) (station locations Fig. 1, data Fig. 2). The monitoring period of the stations was between 1970 and 2000 (varying between stations), and the precipitation monitoring did not overlap with our own sampling.

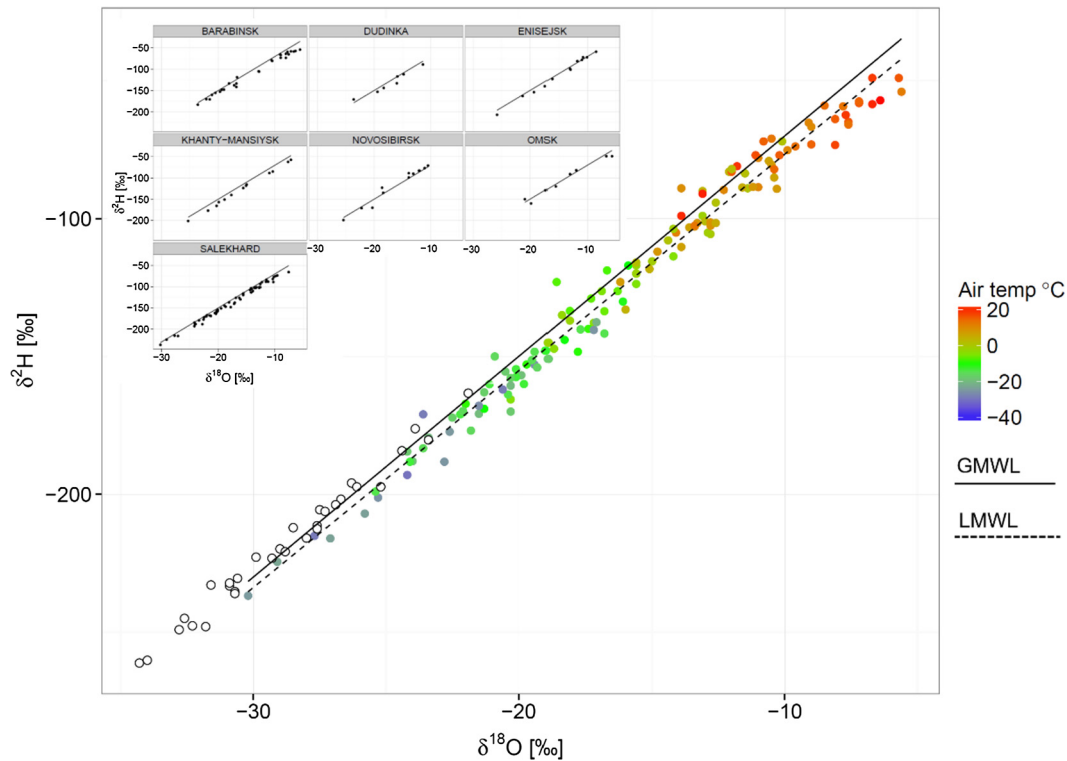


Fig. 2. Precipitation isotope samples from GNIP coloured according to average air temperature of the sampling month to demonstrate seasonality in precipitation. Data from individual stations (see Fig. 1) is shown on the panels in the top left corner. Ground snow samples for isotopes are published in Vasil'chuk et al. (2016). GMWL is the global meteoric water line $\delta^2\text{H} = 8 \cdot \delta^{18}\text{O} + 10$, LMWL is the local meteoric water line derived from GNIP precipitation with the regression equation $\delta^2\text{H} = 7.86 \cdot \delta^{18}\text{O} + 1.9$.

However, the sampling stations envelope our study area in terms of both latitude and longitude, therefore providing baseline information of the typical spatial variability and seasonality of precipitation isotope composition in the WSL.

Vasil'chuk et al. (2016) reported isotopic composition of snow along the same transect as our sampling for February/March of 2014, and full details of the sampling are provided therein and by Shevchenko et al. (2016). We used the data as an additional reference isotopic signature of snow that enters the landscape during snowmelt in 2014.

Data for the discharge and isotopic composition of the river Ob at its outlet (Salekhard, Fig. 1) was produced by the Arctic Great Rivers Observatory (Arctic-GRO) freely available at the portal: www.arcticgreatrivers.org (McClelland et al., 2008). GRO provided flow and isotope data in the Ob was used to contextualize the hydrological regime during our isotope sampling. The discharge at Nikolskoe, located at the mid-reaches of the Ob near where high-frequency isotope sampling took place, was obtained from the Russian Hydrological Service. The discharge at Nikolskoe, where only the water level was measured, was calculated using two adjacent gauging stations where the river discharges are measured: Dubrovino (N 55°28'30,24", E 83°16'44,23", 243 km upstream of Nikolskoe) and Kolpashevo (N 58°18'53,64" E 82°57'00,48", 214 km downstream of Nikolskoe).

2.4. Data analysis

The data were grouped spatially according to the major watersheds having different permafrost regimes; permafrost occurrence is less frequent in the Ob compared to the Pur and Taz (Pokrovsky et al., 2015; Zakharova et al., 2009). To visualise and analyse the temporal variability of isotopes in the area, we grouped the samples according to the seasonality of the hydrological regime;

i.e. winter (Nov-Mar) with baseflow conditions, spring (April-June) with snowmelt influence, and summer/fall (July-Oct) with summer rainfall and evaporation effects (Zakharova et al., 2009). The specific timing of the hydrological regime, e.g. the start of the snowmelt period, vary along the transect because of the long distance between the southern- and northernmost sampling locations, but also between years (Zakharova et al., 2014). This makes the selected time periods somewhat approximate, nevertheless, the sampling of rivers and lakes targets and generally captures these specific periods.

We calculated deuterium excess (d-excess) as $\delta^2\text{H} - 8 \cdot \delta^{18}\text{O}$ (Dansgaard, 1964). Deuterium excess is associated with kinetic isotopic fractionation processes, which are typically indicative of evaporation or condensation. When a d-excess value equals 10, the sample is located on the global meteoric water line (GMWL). Samples with values <10 plot below the GMWL and signal a deviation from the equilibrium fractionation conditions, i.e. the sampled water has been subjected to evaporation (Dansgaard, 1964). D-excess can also reflect different environmental characteristics in precipitation moisture sources (Gat, 1996). We used d-excess as additional index to distinguish between evaporated and non-evaporated stream water sources.

3. Results

3.1. Spatial variability of isotopes

The GNIP precipitation data shows strong seasonality with isotopically depleted samples taken during months with cold air temperature (Fig. 2). Isotopes in the river samples had slightly higher median (−15.3%, values only for $\delta^{18}\text{O}$ are reported) values compared to the median of GNIP precipitation samples (−15.6%), but the variability was significantly lower (interquartile range [IQR]

1.7% in rivers, 8.5% in precipitation) (Fig. 3). Comparing rivers, lakes, and soils, lakes showed the most pronounced enrichment of heavy isotopes (median -11.1%), which was most likely primarily caused by evaporation fractionation but also the influence of more enriched summer precipitation (Fig. 3). Soil solutions were also more enriched (median -13.0%) than rivers, but less than lakes. Snow samples collected by Vasil'chuk et al. (2016) were most depleted (more negative) in heavy isotopes (median -28.8%) and plotted outside the typical values of all other samples (river, soils, lakes), and thereby provided a potentially good tracer for the snowmelt signal in the landscape. The local meteoric water line (LMWL), i.e. the regression line of the GNIP precipitation samples (Fig. 2, Fig. 3), had a slope of 7.86, similar to the GMWL with a slope of 8. The slope of the regression line in all water samples was lower than the LMWL (Fig. 3) in the order of soils (4.64) < lakes (5.54) < rivers (6.08).

There was surprisingly consistent limited change in the river isotope ratios along the transect from south to north (Fig. 4a). Interestingly, instead of a constant, linear south-north depletion along the transect, we found an increased enrichment around the latitude 62°N , best highlighted by the locally weighted least squares regression (LOESS) of the river samples. There seemed to be relatively small latitudinal isotopic differences between lakes and soils. Typically, lakes and soils were more enriched than rivers, but isotopic compositions were overlapping at all latitudes.

As for $\delta^{18}\text{O}$, in the permafrost influenced latitudes ($>60^\circ\text{N}$), variability in d-excess tended to be higher, whereas the samples from lower latitudes were clustering more tightly between 5 and 10‰ (Fig. 4b). There appeared to be decreased levels of d-excess (high evaporation signal) around the latitude 62°N , coinciding with the latitude of increased $\delta^{18}\text{O}$ enrichment. Lakes had high variability and seasonal differences in d-excess at all latitudes. In soil waters, despite the more limited data set, the overall values and variability were similar across the sampled transect.

3.2. Temporal variability of isotopes

Contemporaneous data for both river flow and stable water isotopes in the river Ob are shown in Fig. S1 as a reference for the observed long term variability at the river outlet. River samples from the transect showed higher temporal variability than the Arctic-GRO monitoring at the Ob outlet (Fig. 5 shows Arctic-GRO monthly mean and standard deviation, Fig. S1 presents the full time series). The Arctic-GRO data showed a typical annual cycle of depleted winter/spring and enriched summer values (Fig. 4). This progressive enrichment of streams in our dataset was best seen in the summer of 2015.

Perhaps the most striking finding in the temporal dynamics of our sampled river isotopes was the relatively modest depletion of streams during snowmelt. When the snowpack with a very depleted (negative) isotopic signal (see winter 2013 in Fig. 5) melted in early May, flow in the river Ob outlet was elevated approximately tenfold within less than a month. Despite the substantial flux of depleted snowmelt water, we saw the stream isotope values across the transect changing only slightly (in 2014), if at all (in 2015) towards more depleted signatures.

We used deuterium excess to explore signals of evaporation in the landscape and particularly in the sampled rivers (Fig. 6). The volume weighted average of precipitation d-excess calculated from the GNIP data was 5.2% , which is below the d-excess of the average global meteoric water (10%). In general, the d-excess median for rivers (7.2%) and soils (8.5%) plotted above the median of precipitation d-excess, but, importantly, there were low d-excess values in rivers (i.e. signs of evaporated water, plotting below the average regional precipitation value of 5.2%) not only in the summer, but also during winter and spring in both the Ob and Pur/Taz watersheds (Fig. 6). Snow showed high d-excess values (median 11.8%) typical for the area (Kurita et al., 2005). Lakes had the lowest d-excess values (median -3.4%) with the majority plotting well

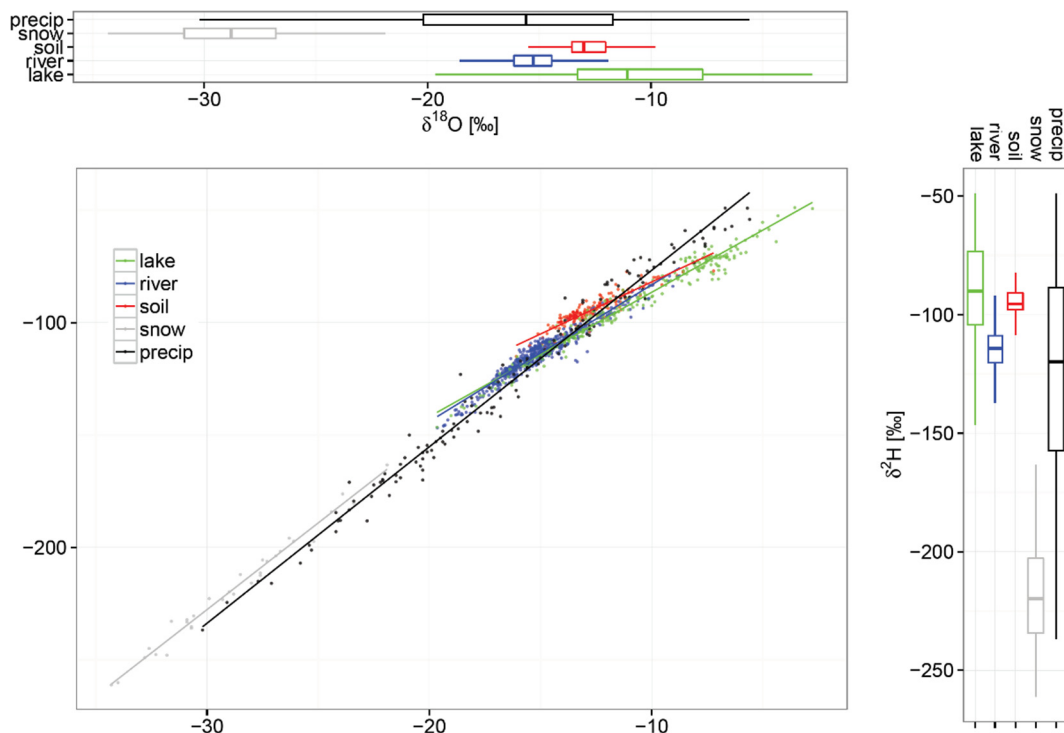


Fig. 3. Dual isotope plot grouping rivers, lakes, soils, snow (Vasil'chuk et al., 2016) and precipitation (GNIP) with different colours and showing distributions as boxplots on side and top panels.

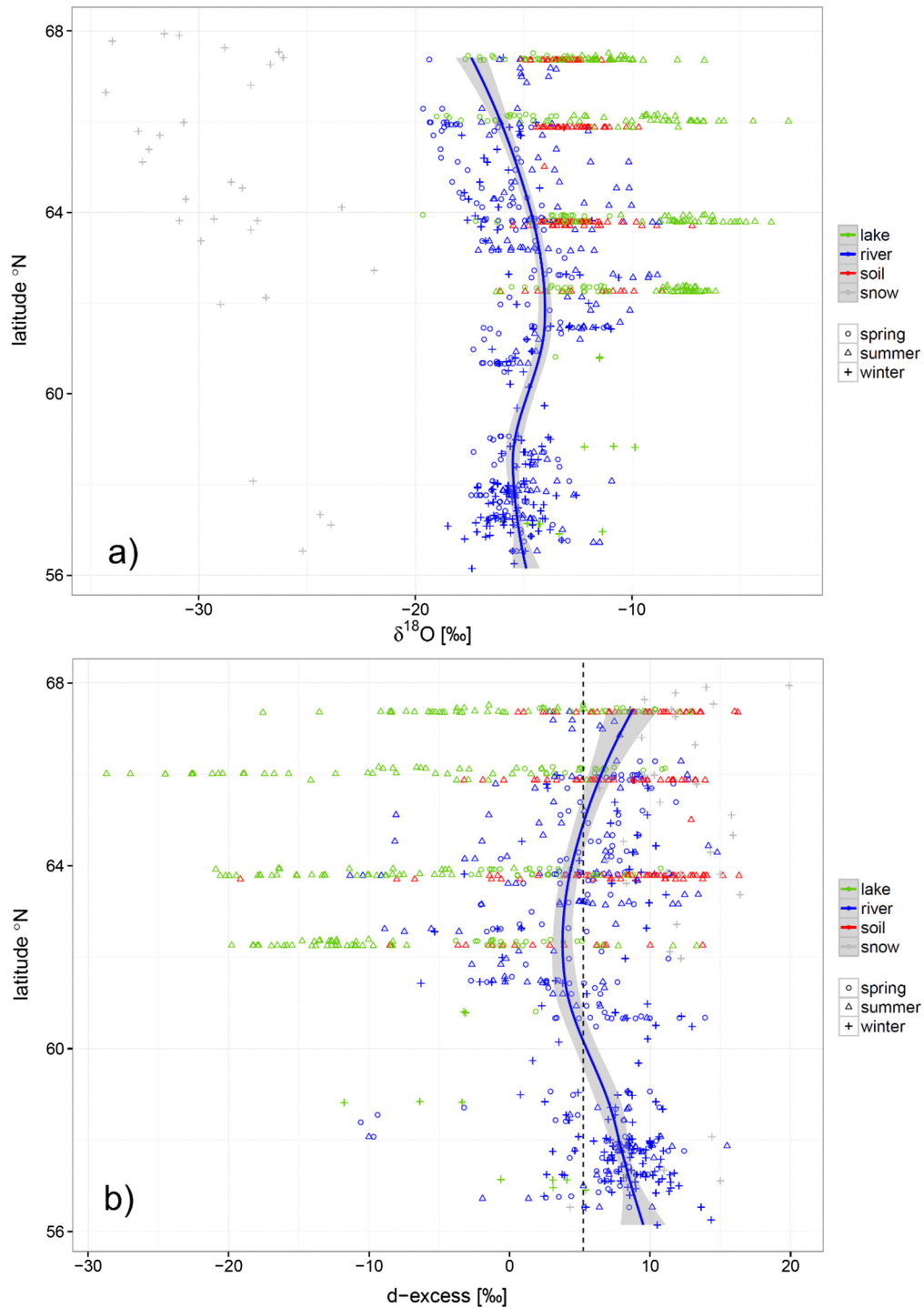


Fig. 4. $\delta^{18}\text{O}$ (a) and d-excess (b) plotted as a function of latitude and grouped by colour to river, lake, soil and snow samples and by symbol to spring, summer and winter seasons. A smoothed average is presented for river samples to show the south-north latitudinal trend, and flow weighted d-excess in precipitation is given as dashed black line.

below the precipitation d-excess indicating a strong evaporation signal (Fig. 6).

High frequency isotope monitoring in the Ob middle reaches at Nikolskoe (Fig. 1) showed elevated levels in $\delta^{18}\text{O}$ and decreased d-excess values coinciding with slightly increased flows in Nov-Dec 2015 (Fig. 7). As winter progressed, there was a steady decline in $\delta^{18}\text{O}$ during baseflow from January until March, moving gradually from enriched (evaporated water and summer precipitation) to a more depleted water source, likely from the well mixed

deeper groundwater. The d-excess of the river plateaued near the value of 10‰, i.e. into a water source with minimal evaporation signal. Surprisingly, at the start of snowmelt in late March there was a relatively minor shift of depletion in $\delta^{18}\text{O}$ from isotope composition between -15 and -16% to values between -16 and -17% . The water in the river during flood stage was not reflecting the isotopic composition of melted snow (depleted in $\delta^{18}\text{O}$). Starting late April, after the snowmelt, the stream isotopes start to gradually turn more enriched with some peaks during high flows (see

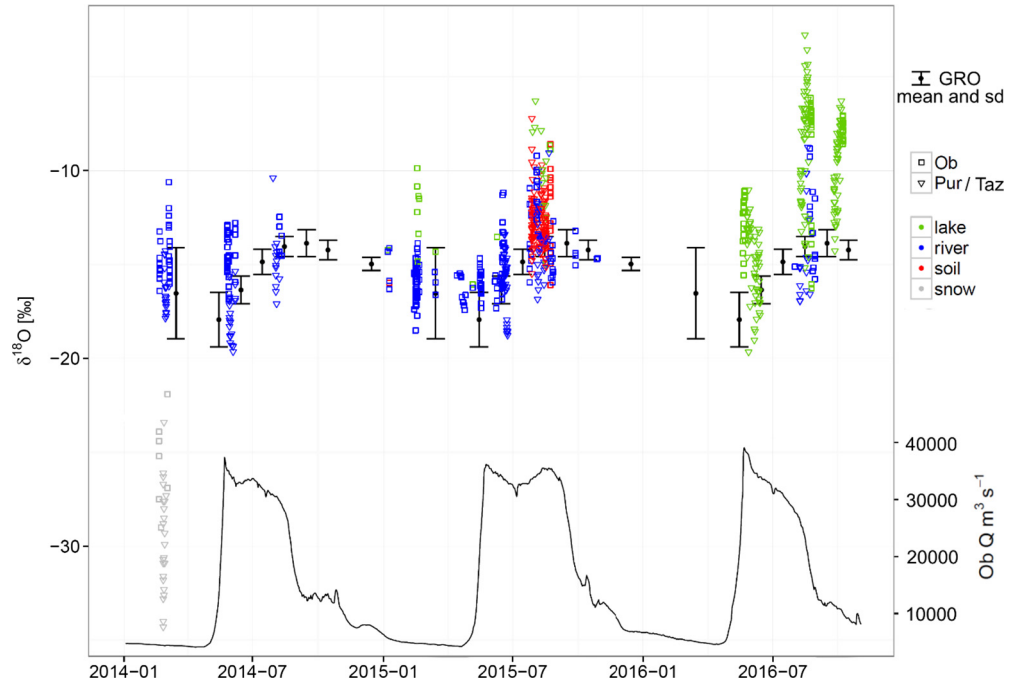


Fig. 5. Time series of $\delta^{18}\text{O}$ samples grouped by colour to river, soil, lake, and snow samples and by symbols to the Ob and Pur/Taz watersheds. Long term monthly mean and standard deviation of $\delta^{18}\text{O}$ and discharge at the Ob outlet (Arctic-GRO) are provided for reference.

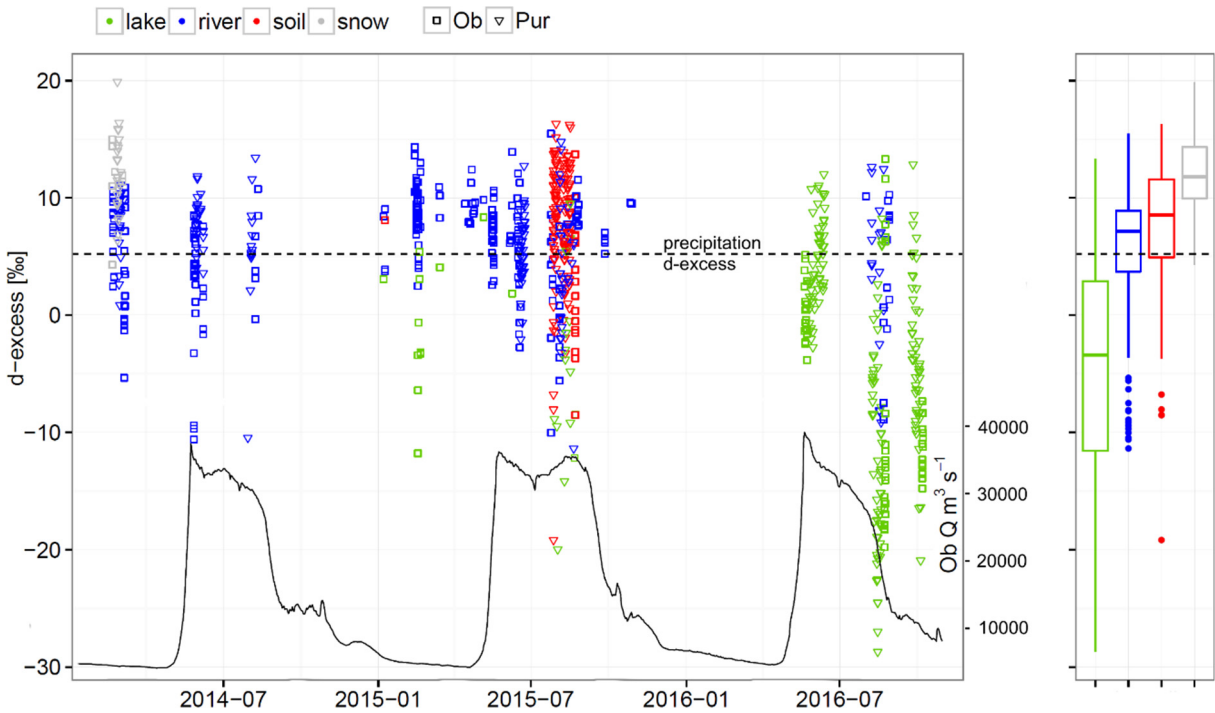


Fig. 6. Time series for d-excess grouped to river, soil and lake samples according to colour, and Ob and Pur watersheds according to symbol. Side panel shows the distribution of the samples as boxplots. Volume-weighted mean of GNIP precipitation d-excess is 5.2%, shown as a horizontal line.

e.g. start of May). The peaks in isotopic enrichment in open water season are typically associated with low d-excess values (Fig. 7).

3.3 Water sources in the WSL inferred from temporal and spatial variability in isotopes When disaggregating the samples according to watersheds and hydrological seasons, sites from the more northern Pur/Taz watersheds tended to have more depleted $\delta^{18}\text{O}$ signatures than the southern reaches of the Ob in all seasons

and in all water bodies (Fig. 8a). In river samples, there was a general isotopic evolution from depleted spring values, to enrichment over the summer and a return to a more depleted level in the winter. The observation that the spring snowmelt (snow being depleted) did not lead to substantial isotopic depletion in the streams is also evident in Fig. 8a, as the spring and winter medians were very similar in both watersheds.

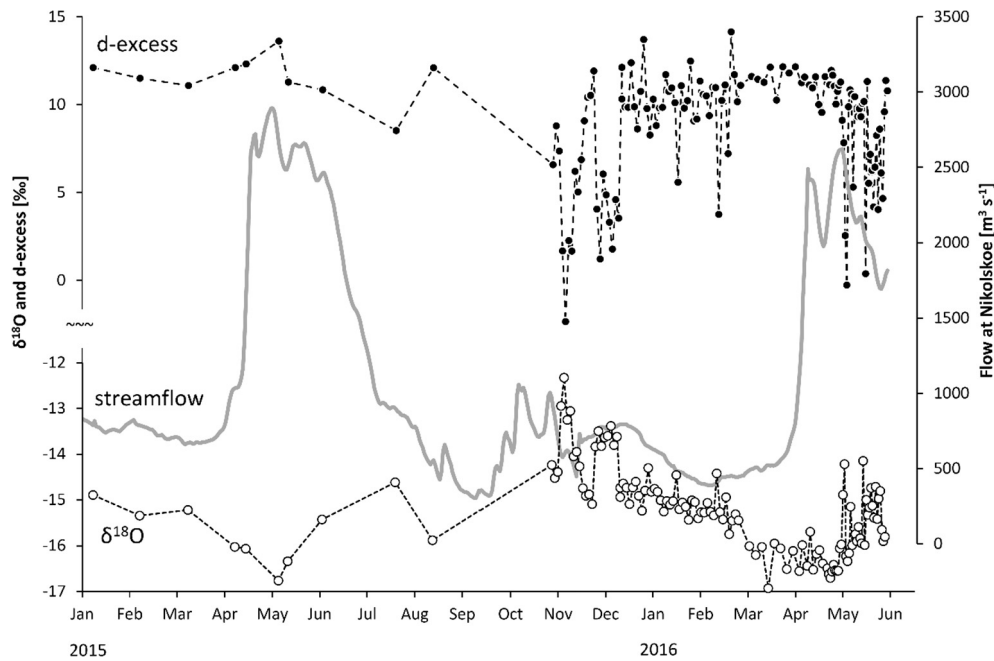


Fig. 7. $\delta^{18}\text{O}$, d-excess and flow time series from continuous sampling at Nikolskoe, mid-Ob (see Fig. 1).

Rivers exhibited notably low differences in d-excess between seasons and watersheds (Fig. 8b), with only minimally decreased levels (increased evaporation signal) in the summer. Lakes and soils showed differences in d-excess both (1) between watersheds, with more clear evaporation signals (lower median in d-excess values) in the Ob, and (2) between seasons with lowest d-excess during summer, though seasonality was most clearly evident in the lakes which may also reflect the more temporally extensive sampling.

4. Discussion

4.1. Spatial variability of isotopes

The spatial and temporal extent of our stable water isotope dataset is rare, even when compared to work in more temperate climates (e.g. Jasechko et al., 2017). With such a dataset, we are in a position to begin to bridge the gap between understanding gained from isotope studies in large Pan-Arctic watershed outlets (Cooper et al., 2008; Welp et al., 2005; Yi et al., 2010; Yi et al., 2012) and smaller scale studies (Hayashi et al., 2004; Song et al., 2017; Streletskiy et al., 2015; Throckmorton et al., 2016) to better understand runoff generation and water sources in permafrost-influenced lowland areas with extensive lake and wetland coverage. In North America, Lachniet et al. (2016) sampled rivers and Gibson (2001) lakes at scales similar to ours, providing information on isotopic variability in high-latitude landscapes. However, these were confined to shorter monitoring periods and single waterbody type (rivers or lakes) constraining the development of a more integrated conceptualisation of northern large scale hydrology.

The expected damped variability of isotopes in rivers compared to precipitation (Fig. 3) indicates mixing of rainfall/snowmelt with stored water within the landscape as it traverses the sampled catchments. The more enriched median in rivers indicates a preferential sourcing of river water from isotopically heavier summer precipitation (Fig. 2) and/or water enriched by evaporation from storage in the landscape, rather than winter precipitation in the form of snowmelt. The slope of the regression line in all water samples was lower than the LMWL (Fig. 3) in the order of soils < lakes

< rivers, which can be interpreted as an evaporation signal in all waterbodies, with slope of the lines agreeing with global analysis by Gibson et al. (2008).

The more northern Pur/Taz watersheds were isotopically more depleted compared to the middle reaches of the Ob (Fig. 8a). This was likely related to the isotopic composition of precipitation, which is typically more depleted in northern latitudes due to colder air temperatures. Even so, according to one-way Analysis of Variance test, the GNIP stations (station locations in Fig. 1, data in Fig. 2) did not differ in their mean values for precipitations isotopes (at the significance level of 0.05). The GNIP data, even though collected before our study, suggests that the isotope variability in precipitation along either north-south or east-west gradient is not a decisive factor in the isotope variability in the WSL. In comparison, Lachniet et al. (2016) reported a $-8.3\%/1000\text{ km}$ south-north gradient for rivers in the Yukon and Alaska. The lower south-north gradient in the WSL was likely a result of the low elevation with less orographic distillation, and major water vapour sources shifting temporally between the Atlantic and the Pacific oceans reducing the continentality effect in precipitation along the transect (Kurita et al., 2005).

The lakes and soil water in the WSL typically had an enriched isotope signal (Fig. 3), but lakes were most clearly distinguished by their low d-excess values (Fig. 6). Previous work found similar isotopic enrichment of high-latitude lakes in North America and used it to estimate evaporation rates from lakes or entire catchments (Gibson, 2001; Narancic et al., 2017). The WSL has been shown to have anomalously high evaporation rates compared to other high-latitude watersheds because of the high percentage of lake and wetland cover and, therefore, water available for free water evaporation (Serreze et al., 2002; Zakharova et al., 2014). In further work, our dataset will be used to analyse evaporation rates in the very shallow lakes (typically 0.5–1.5 m) across the WSL at the four sites that were intensively monitored in 2016.

Our soil sampling focused on summer because the soil is generally frozen from September – July, and we can therefore say less about the seasonality (differences between the frozen and thawed state) of soil water isotopes than those of lakes and rivers. Nevertheless, the spatial extent of our soil water sampling in the

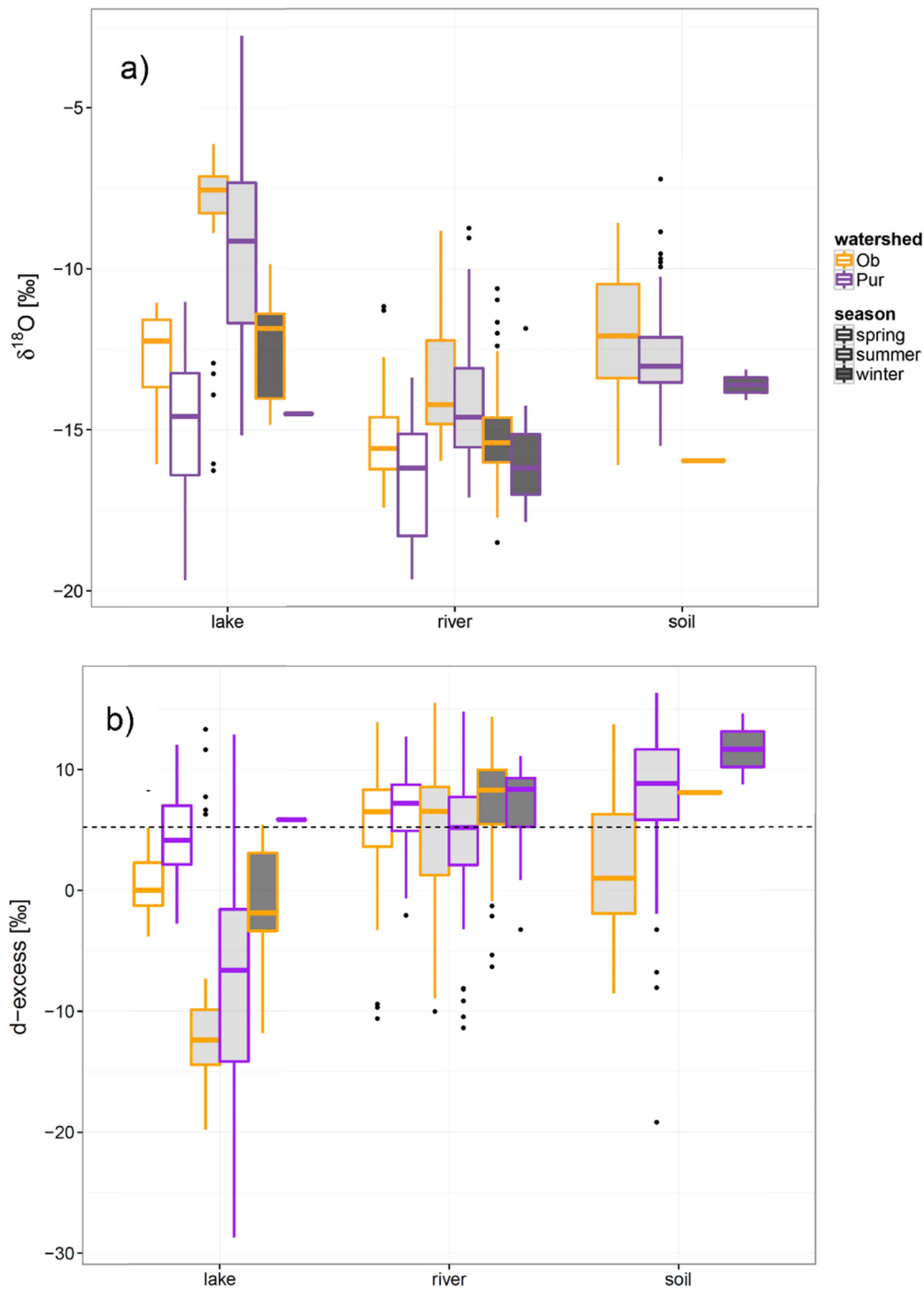


Fig. 8. Boxplots showing the distribution of $\delta^{18}\text{O}$ (a) and d-excess (b) when data are grouped to sampled water body, major watershed and sampling season.

high-latitude environments is unusual, as prior work has been looking at soil isotope variability in plot, hillslope or small catchment scale (Carey and Quinton, 2004; Peralta-Tapia et al., 2015; Streletskiy et al., 2015; Throckmorton et al., 2016). Based on the higher intercept of the regression line (Fig. 3), soil water samples appear to be more clearly sourced by enriched summer precipitation than lakes and rivers. In July 2015 when soils, rivers and lakes were sampled during the same time period, the soil isotopes cluster in the same range as the rivers and lakes (Figs. 5 and 6), pointing to a hydrological connection between the three in the WSL as suggested by Zakharova et al. (2014). Typically, lakes and soils were more enriched than rivers (Fig. 3), but isotopic compositions

were overlapping at all latitudes (Fig. 4), suggesting common sources and connectivity in some of the sampled tributaries.

As a result of permafrost thaw, high-latitude watersheds are expected to shift towards more groundwater dominated systems with deeper active layers (Evans and Ge, 2017; Frampton and Destouni, 2015). In terms of the isotopic variability in rivers, this would be manifested in greater damping due to the lower influence of frozen soils generating overland flow (and rapid transmission of a snowmelt isotope signal) and greater mixing in the thawed subsurface. In our data, isotopic variability in spring snowmelt in the Taz/Pur ($>63^\circ\text{N}$) watersheds with strong permafrost influence is greater than in the Ob watershed ($<63^\circ\text{N}$) (Fig. 8a) with

weaker permafrost influence, which can be interpreted as subtle evidence of permafrost-influenced hydrological routing of the depleted snowmelt water to streams more quickly in more northern catchments.

However, the presence of permafrost is difficult to map for large areas (Walvoord and Kurylyk, 2016; Woo et al., 2008), and other categorizations than the primary watershed could have been selected. In our study, the samples taken south of $\sim 60^\circ\text{N}$ would be most likely to be in the permafrost free zone (Fig. 1). If comparing the variability south and north of 60°N (Fig. 4), the rivers in permafrost free areas ($<60^\circ\text{N}$) do appear to be less variable in both $\delta^{18}\text{O}$ and d-excess and cluster more tightly together. Higher latitudes more influenced by permafrost ($>60^\circ\text{N}$), showed more distinct separation between spring, winter and summer samples. This makes a stronger case for permafrost increasing the isotopic variability than seen in Fig. 8, which could be inferred as more rapid surface flow component in the northern than the southern parts of the WSL.

More catchment specific analysis considering attributes such as air temperature, relative humidity, permafrost coverage, lake, forest and bog proportion on the watershed (as in Pokrovsky et al., 2015; Zakharova et al., 2014) is needed to better understand the reasons for spatial isotope variability in the WSL. However, the additional analysis are beyond the scope of the current this work, and will be addressed in our future research.

4.2. Temporal variability of isotopes

Both of our datasets – the high frequency sampling of the middle Ob (Fig. 7) and spatial sampling along the transect (Fig. 5) – showed a strikingly modest signal of isotopic depletion in rivers during snowmelt. The isotopic snowmelt signal in high-latitude rivers varies: a clear snowmelt depletion signal ($>3\%$) is typical in permafrost dominated mountain-fed catchments (McNamara et al., 1997; Streletskiy et al., 2015; Welp et al., 2005), or in snow-influenced environments in general (Taylor et al., 2002). In a study encompassing a similar spatial scale to ours (Welp et al., 2005) stable water isotopes were used to calculate that the winter precipitation (snowmelt) accounts for $\sim 60\%$ of flow in the arctic $650,000\text{ km}^2$ watershed of Kolyma, northeast Siberia underlain by continuous permafrost. In the Yukon and Alaska Lachniet et al. (2016) reached similar conclusions of snowmelt dominance as they did not find a warm season precipitation isotope signal in their river transect ranging from permafrost free to continuous permafrost.

Our data indicate a contrasting situation in the WSL, where a depleted river signal from snowmelt is not obvious (Figs. 5 and 8). A likely explanation is that there is a high mixing volume in lakes, wetlands, and soils in the WSL to absorb and substantially mix the pulse of depleted snowmelt runoff before it reaches the streams. Furthermore, the river isotope composition is leaning towards being more enriched, suggesting snowmelt primarily displaces precipitation inputs from the previous summer and/or evaporated waters (Fig. 3), similar isotope-based work by Yi et al. (2010) and Gibson et al. (2016) also suggests large wetland influence in the runoff generation in the Athabasca and Mckenzie rivers systems in Canada. The long term monitoring by Arctic-GRO (Fig. S1) generally supports this, showing a gradual depletion of the Ob isotopic composition over the winter similar to the one seen in Fig. 7 (winter 2012/2013 in Fig. S1 shows the clearest example having the most data points). During the entire 10 years of Arctic-GRO isotope data, a sudden depletion during/after snowmelt occurred only in 2015. According to long term monitoring by Russian Hydrological Survey at the Ob River middle course, spring of 2015 experienced an anomalously high flood with a

return period of 20–40 years. However, from our data depletion from snowmelt was not substantial in 2015 (Fig. 5).

When the data were grouped according to seasons and watersheds (Fig. 8a), we observed that the median in $\delta^{18}\text{O}$ is remarkably similar for winter baseflow and spring snowmelt in both watersheds with strong and weak permafrost influence. Contrasts in topography and permafrost extent provide potential explanations for the different snowmelt depletion in the WSL compared to other large scale isotope studies in high-latitude catchments. The transect of Lachniet et al. (2016) in Alaska had greater topographic variability. Steeper slopes are prone to promote surface flow from snowmelt runoff (Woo, 1986). The Kolyma watershed studied by Welp et al. (2005) is completely underlain by permafrost, which is also likely to lead to more marked, less mixed snowmelt runoff compared to lower permafrost influence (Carey and Quinton, 2004; Streletskiy et al., 2015). Nonetheless, Zhou et al. (2015) used isotopes for hydrograph separation at the Shule River Basin ($14 \times 10^4\text{ km}^2$) at the Tibetan Plateau; a mountainous watershed with $>80\%$ permafrost coverage, and found a strong groundwater dominance.

4.3. Water sources in the WSL inferred from temporal and spatial variability in isotopes

Stable water isotope techniques have revolutionised the understanding of how water is stored and released in the environment (Kendall and McDonnell, 1998). Most geographic and climatic regions, from headwaters to continental watershed scales, exhibit damping of the isotope signal from precipitation to streamflow, confirming substantial storage and mixing of water in the runoff generation process (McGuire et al., 2005; Jasechko et al., 2016). In comparison to temperate regions, where most isotope work has been done, work in snow-influenced areas has shown the important presence of snowmelt water in streams by typically reporting depleted steam isotope composition during snowmelt (Taylor et al. 2002; Tetzlaff et al., 2015b). Frozen soil (seasonal and permafrost) intuitively promotes the rapid routing of snowmelt in the landscape by blocking infiltration (Carey and Quinton 2004; Woo et al., 2008), but firm conclusions on this has been difficult to establish on catchment scales with isotope data (Carey and Quinton, 2004; Lindström et al., 2002; Song et al., 2017).

The multi-year isotope sampling in the WSL allowed us to develop an integrated conceptual model of the dominant runoff generation processes during all main hydrological seasons (winter, spring snowmelt, summer), and to hypothesise likely transient hydrological connections in this vast lowland area influenced by permafrost (Fig. 9). Previous large scale hydrological work focused on the WSL has been successful in isolating volumetric contributions of snowmelt, groundwater, summer rainfall, and evaporation and finding relationships with seasonal water balance components and climatic variables (Novikov et al., 2009; Serreze et al., 2002; Yang et al., 2004; Ye et al., 2004; Zakharova et al., 2009; Zakharova et al., 2011; Zakharova et al., 2014). However, it has not been possible to assess the dynamics of hydrological connectivity and storage in the WSL, which is crucial to better understand and link hydrological and biogeochemical processes. This is because the release of C and other elements from high latitude landscapes is intimately controlled by the interactions between temperature, soil thaw and permafrost melt (see Section 4.4 below).

Previous work in the WSL and similar wetland-influenced high-latitude watersheds suggests great potential for the landscape to mix and store high volumes of snowmelt water, which we hypothesise to cause the modest isotopic depletion during snowmelt. Work in the WSL by Zakharova et al. (2011) used hydrometric data and remote sensing estimates of spatially distributed snow cover,

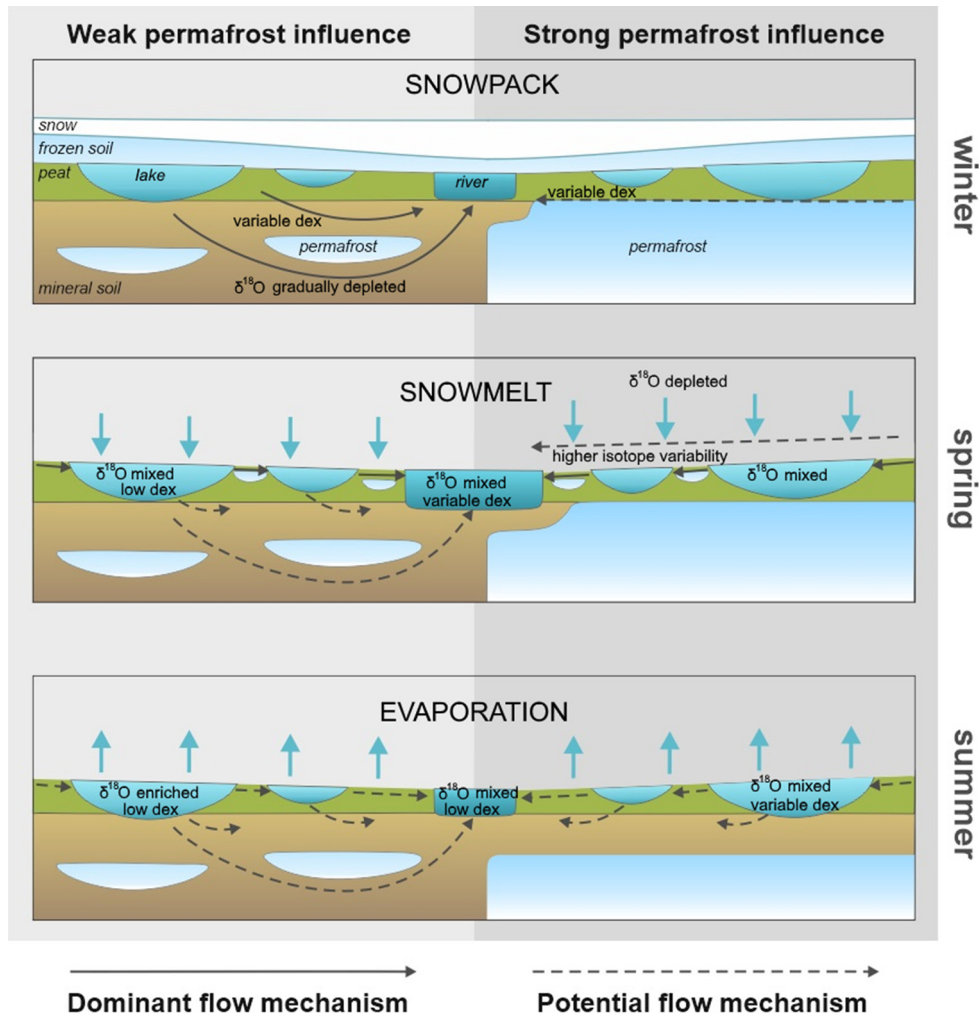


Fig. 9. Based on our isotope data, we conceptualised runoff generation processes in the WSL for different hydrological seasons and for areas with weak and strong permafrost influence, presented in cross-sections. During the snow cover period, the d-excess (dex, signal of evaporation) in winter baseflow suggests a hydrological connection between the unfrozen active layer and the wetlands, and rivers. During spring, the isotopically depleted snowmelt signal is largely missing from rivers while the rivers are still displaying varying degrees of dex (evaporation) signal. We propose that the snowmelt water is mixed with water stored in lakes and the active layer and displaced to rivers. Higher isotopic variability for permafrost areas in the spring points towards the capability of permafrost soils for more rapid routing of water. In the summer, there is a hydrological connection between lakes, active layer, and rivers, where the persistent but variable dex signal in rivers across the transect suggests a range of hydrological connectivities from near-surface to subsurface dominated.

concluding that on average 30% of snowmelt water was retained in the lakes and wetlands during the year of melt. Further, [Zakharova et al. \(2014\)](#) quantified that the permafrost free area of WSL has a wetland storage variation 1.5–2.5 times the annual runoff, with a lower storage capacity of 0.5 times annual runoff in the permafrost zone. [Smith et al. \(2012\)](#) used peat soil core analysis and GIS data to reach similar water storage estimates of 3 times the Ob annual runoff in the WSL peatlands. When the [Smith et al. \(2012\)](#) estimate of 2000 mm water storage (in watershed averaged water equivalent) is compared with the typical snow water equivalent 200–250 mm of in the northern WLS ([Zakharova et al., 2011](#)), there is clearly sufficient storage capacity for snowmelt mixing – assuming that this storage is available the onset of snowmelt. Common understanding is that this storage would be frozen during snowmelt, particularly so in permafrost-affected regions, but our isotope data suggests that in fact a substantial fraction of the surface storage is available to mix the isotopically depleted snowmelt signal. Other isotope work in boreal catchments has shown that wetlands acts as ‘isostats’ ([Tetzlaff et al., 2014](#)) where the water storage in the wetlands mixes and damped diverse, temporally variable source waters to “set” the river isotope compositions

([Lessels et al., 2016](#)). This has been quantitatively supported by subsequent isotope based modelling studies ([Soulsby et al., 2015](#)).

In northern Alaska, [Bowling et al. \(2003\)](#) found that 25–50% of annual snowmelt was needed to fill the storage deficit caused by evaporation in the previous year. Substantial isotopic mixing of snowmelt in lake/wetland dominated systems was also documented in the MacKenzie basin, Canada, where [Hayashi et al. \(2004\)](#) used isotopes and hydrometric measurements to show how lake-wetland complexes hydrologically connect to streams during snowmelt and how >50% of the stream water during snowmelt originated from water stored in lakes and wetlands over winter. These percentages generally point to volumes of snowmelt that does not contribute to runoff in the short-term, i.e. water either stored or evaporated during the snowmelt period. Our data suggest that the landscape in the WSL is not only a sink for the snowmelt water, but has great capacity to mix water in lakes and wetlands before it reaches the streams.

Surface hydrological connections between streams, lakes and wetlands in permafrost landscapes are established and disconnected dynamically and quickly after rainfall and/or snowmelt ([Bowling et al., 2003](#); [Hayashi et al., 2004](#); [Quinton and Roulet,](#)

1998). Smith and Alsdorf (1998) used remote sensing (SAR-data) to show how 90% of the lakes in the river Ob floodplain near Salekhard were up to 90% hydrologically connected to the river at the peak of snowmelt, with a rapid decline in connectivity as the flows subsided. Analysis in Zakharova et al. (2014) showed how the maximum wetted area in catchments in the WSL typically reaches ~80% in the spring after snowmelt and subsequently recedes to fractions between 80 and 20% throughout the growing season, depending on the hydrological regime. In our study, lakes and soils typically had an enriched isotope signal and a distinctly negative d-excess. We therefore hypothesise that rivers showing signs of low d-excess values are hydrologically connected to lakes and/or wetlands (Lachniet et al., 2016; Streletskiy et al., 2015).

Indeed, we found a low d-excess values in the streams in all seasons and across latitudes (Fig. 8b), suggesting an active/ongoing hydrological connection in several rivers from evaporated water residing in lakes. The dynamic surface connection and low d-excess values after rainfall events in our data was evident in the high-frequency monitoring of the Ob at Nikolskoe (Fig. 7). The low d-excess values occurring with the elevated $\delta^{18}\text{O}$ during autumn rainfall events (Nov-Dec 2015) suggested evaporated water sourcing the stream; this is more likely to originate from water displaced from the landscape than the incoming rainfall. Similarly, Yi et al. (2012) observed an enriched isotope signal at the Ob outlet during normal summer flows and attributed this to mixture of groundwater, summer precipitation and water stored in the wetlands sourcing the summer flows in the Ob. We even saw low d-excess values in some of the rivers immediately after snowmelt (Fig. 6), suggesting snowmelt mixing with and displacing water stored in the lakes and soils over winter, as shown by Hayashi et al. (2004) using water isotopes in a similar landscape Mckenzie basin in Northern Canada.

In addition to the dynamic activation of surficial hydrological connectivity, subsurface connections are known to exist in permafrost-influenced catchments either in supra-permafrost active layer, or deeper, sub-permafrost groundwater flow and taliks (Woo, 1986), and their importance is expected to increase with thawing permafrost (Frampton and Destouni, 2015; Walvoord and Kurylyk, 2016). Our data suggests a persistent connection between rivers and the landscape, as rivers carry water with an evaporated signal (low d-excess) in all seasons, including winter (Fig. 6, Fig. 8b). Furthermore, the similarity in d-excess in the Pur/Taz and Ob watersheds suggests a similar degree of connectivity between rivers and the landscape in watersheds with weak and strong permafrost influence, and also for all seasons, which was an unexpected finding (Fig. 8b). Streletskiy et al. (2015) hypothesised similar over-winter hydrological connection in the unfrozen active layer in a 320 km² catchment in discontinuous permafrost in the northern part of the Yenisey watershed in Siberia, where they documented low d-excess values in winter baseflow. Yang et al. (2017) found close hydrological connections between river, thermokarst lakes and degrading permafrost at the Beiluhe Basin, Qinghai-Tibet Plateau using stable water isotopes.

It should be noted that because of the spatial extent of the sampling campaigns (see Fig. S2) and associated logistical challenges, the temporal variability along the transect inevitably remains somewhat uncertain. Some areas are less intensively sampled, which may cause biases in the analysis of spatial and temporal variability. Therefore, our interpretation of the isotopic variability is necessarily preliminary in nature, and the patchy nature of the sampling precludes robust statistical testing the different seasons or waterbodies. In addition, in the absence of rain samples from the events during our monitoring period, uncertainty in the source of water with low d-excess remains, because rainfall can also carry a low d-excess signal varying with precipitation moisture sources

(Gat, 1996). Nevertheless, the data set remains useful and an evidence base for the inferences drawn and subsequent hypothesis testing.

4.4. Wider implications

An interesting finding was that both the d-excess and $\delta^{18}\text{O}$ values in rivers peaked around 62°N (Fig. 4), instead of decreasing (for d-excess) or increasing (for $\delta^{18}\text{O}$) linearly towards southern latitudes with higher evaporative potential and enriched precipitation, respectively. Both the GNIP precipitation isotope data and Kurita et al. (2005) suggest that this anomalous variability is not caused by persistent patterns of oceanic moisture sources. Instead, we propose that the increase around 62°N could be caused by an intensified hydrological significance of lakes and wetlands, because their abundance is highest around the same latitudes (Pokrovsky et al., 2016; Zakharova et al., 2014). This hypothesis requires further research examining catchment specific lake and wetland percentages, which is beyond the scope of this work. Influence of climate change in permafrost hydrology has been primarily viewed from the perspective of active layer development, and the resulting longer subsurface flow paths leading to longer water residence times (Walvoord and Kurylyk, 2016). If the importance of lakes in sourcing stream flow can be shown, that would provide further evidence that the changes observed in the lake abundance in the high-latitude regions (Quinton et al., 2011; Smith et al., 2007b) caused by climate change are likely to have profound hydrological consequences on stream water sources.

Our study also points towards high storage and mixing volumes in the landscape, which increase residence time and would imply a damped and delayed response of rivers to biogeochemical processes such as contamination and accelerated nutrient cycling. However, with the observed persistent hydrological connectivity between landscape and rivers (Fig. 9), solutes such as DOC could be delivered to streams all year round, likely with peaks during snowmelt (Avagyan et al., 2016; Giesler et al., 2014) when the water stored in the landscape is displaced to rivers. Frey and Smith (2005) found that higher peatland percentage increases the DOC flux in the WSL, but only in permafrost free catchments. They propose two explanations for lower DOC export from permafrost catchments: (1) DOC transport is restricted by the permafrost creating a physical barrier to infiltration and hydrological connectivity; this confines DOC generation and transport to shallow active layer. Or, (2) the DOC increases in lower latitudes are driven by higher air temperatures causing elevated DOC production. Our work suggests a hydrological connection between the landscape and rivers, in both permafrost conditions, so the latter explanation for higher DOC export in Frey and Smith (2005) from permafrost free catchments may be more likely. Future temperature increases, with increased melt in permafrost regions is likely strengthen such connectivity and DOC release. The potential implications for subsequent degassing of CO₂ from lakes and rivers, and associated CH₄ release from wetland areas are beyond the scope of the current study, but are important in terms of the global carbon budget (Cole et al., 2007).

Tracer-aided models adjusted to northern snow-influenced conditions (Ala-aho et al., 2017; Fekete et al., 2006; Smith et al., 2016; Tetzlaff et al., 2015a) could utilize long term datasets with good spatial coverage, like the one we present in this work, to hypothesis development and testing. Hydrological model development for permafrost areas is a persistent challenge in regions with sparse data and few suitable simulation codes (Bowling and Lettenmaier, 2010; Walvoord and Kurylyk, 2016). In particular, more continuous sampling of rivers has the potential to reveal activation of hydrological connections (like in Fig. 9) and could provide valuable data for hydrological parametrisation and modelling.

5. Conclusion

The unprecedented spatio-temporal scale of our stable water isotope sampling in the Western Siberian lowlands (WSL) allowed an improved conceptual understanding of dominant runoff generation processes and the hydrological connectivity in this wetland and permafrost-influenced landscape. Our findings suggest significant surface water storage capacity in the WSL is involved in intensive isotopic mixing of snowmelt water and dictates that only a relatively small proportion of the water molecules released from melting snow contributed to rivers flow during the spring. Based on this, and the isotopic evaporation signal (low d -excess value), we hypothesise that the primary runoff generation mechanism in WSL is the displacement of water already stored in the lakes, wetlands and soils to rivers as shallow subsurface flow and supra-permafrost flow. Also, the isotope evaporation signal suggests that even in snow-covered winter baseflow period, many rivers in the WSL remain hydrologically connected by drainage from the surrounding lakes and wetlands in the landscape. There were some, but surprisingly limited, evidence of permafrost causing short-circuiting of less well-mixed snowmelt rapidly to rivers, but this permafrost influence in the WSL needs additional research. The improved conceptual understanding of the runoff generation and hydrological connectivity gained in this work is important framework that can be tested with modelling and provides insights relevant to future pathways of solute and sediment mobilisation as a result of rapid climate change in the WSL.

Acknowledgements

The research has been supported by the NERC/JPI SIWA project (NE/M019896/1); the Swedish Research Council grant No 325-2014-6898; grant issued in accordance with Resolution of the Government of the Russian Federation No. 220 dated 9 April 2010, under Agreement No. 14.B25.31.0001 with Ministry of Education and Science of the Russian Federation dated 24 June 2013 (BIO-GEOCLIM); grant RFBR No 17-05-00-348a; grant FCP “Kolmogorov” 14.587.21.0036, grant RNF No 15-17-1009, and grant RFBR No 17-55-16008.

Stable water isotope data are available in the Natural Environment Research Council (NERC) Environmental Information Data Centre (EIDC) data repository (title: “Stable water isotopes in Western Siberian inland waters”, permanent identifier: <https://doi.org/10.5285/ca17e364-638d-4949-befb-b18b3770aec6>). We would like to acknowledge the Arctic-GRO and IAEA for their publicly available databases providing supporting data for our analyses. Stream flow data at Nikolskoe was provided by Sergey Vorobiev. Liliya Kovaleva is acknowledged for the artwork in Fig. 9. We would like to thank the two anonymous reviewers and the handling editors for their constructive comments that improved the manuscript.

Appendix A. Supplementary data

Supplementary data associated with this article can be found, in the online version, at <https://doi.org/10.1016/j.jhydrol.2017.11.024>.

References

Ala-aho, P., Tetzlaff, D., McNamara, J.P., Laudon, H., Soulsby, C., 2017. Using isotopes to constrain water flux and age estimates in snow-influenced catchments using the STARR (Spatially distributed Tracer-Aided Rainfall-Runoff) model. *Hydrol. Earth Syst. Sci. Discuss.* <https://doi.org/10.5194/hess-2017-106>.

Avagyán, A., Runkle, B.R., Hennings, N., Haupt, H., Virtanen, T., Kutzbach, L., 2016. Dissolved organic matter dynamics during the spring snowmelt at a boreal river

valley mire complex in Northwest Russia. *Hydrol. Process.* 30, 1727–1741. <https://doi.org/10.1002/hyp.10710>.

Bintanja, R., Seltens, F.M., 2014. Future increases in Arctic precipitation linked to local evaporation and sea-ice retreat. *Nature* 509, 479.

Bowling, L.C., Kane, D.L., Gieck, R.E., Hinzman, L.D., Lettenmaier, D.P., 2003. The role of surface storage in a low-gradient arctic watershed. *Water Resour. Res.* 39, 1807. <https://doi.org/10.1029/2002WR001466>.

Bowling, L.C., Lettenmaier, D.P., 2010. Modeling the effects of lakes and wetlands on the water balance of Arctic environments. *J. Hydrometeorol.* 11, 276–295. <https://doi.org/10.1029/2002WR001466>.

Brown, J., Ferrians O., Heginbottom J.A., Melnikov E., 2002. Circum-Arctic Map of Permafrost and Ground-Ice Conditions, Version 2, Boulder, Colorado USA. NSIDC: National Snow and Ice Data Center. Date Accessed 24 April 2017.

Carey, S., Quinton, W., 2004. Evaluating snowmelt runoff generation in a discontinuous permafrost catchment using stable isotope, hydrochemical and hydrometric data. *Hydrol. Res.* 35, 309–324.

Cole, J.J., Prairie, Y.T., Caraco, N.F., McDowell, W.H., Tranvik, L.J., Striegl, R.G., Duarte, C.M., Kortelainen, P., Downing, J.A., Middelburg, J.J., Melack, J., 2007. Plumbing the global carbon cycle: integrating inland waters into the terrestrial carbon budget. *Ecosystems* 10, 172–185.

Cooper, L.W., McClelland, J.W., Holmes, R.M., Raymond, P.A., Gibson, J., Guay, C.K., et al., 2008. Flow-weighted values of runoff tracers ($\delta^{18}\text{O}$, DOC, Ba, alkalinity) from the six largest Arctic rivers. *Geophys. Res. Lett.* 35, L18606. <https://doi.org/10.1029/2008GL035007>.

Coplen, T.B., 1994. Reporting of stable hydrogen, carbon and oxygen isotopic abundances (technical report). *Pure Appl. Chem.* 66, 273–276.

Dansgaard, W., 1964. Stable isotopes in precipitation. *Tellus* 16, 436–468.

Evans, S.G., Ge, S., 2017. Contrasting hydrogeologic responses to warming in permafrost and seasonally frozen ground hillslopes. *Geophys. Res. Lett.* 44, 1803–1813. <https://doi.org/10.1002/2016GL072009>.

Fekete, B.M., Gibson, J.J., Aggarwal, P., Vörösmarty, C.J., 2006. Application of isotope tracers in continental scale hydrological modeling. *J. Hydrol.* 330, 444–456. <https://doi.org/10.1016/j.jhydrol.2006.04.029>.

Frampton, A., Destouni, G., 2015. Impact of degrading permafrost on subsurface solute transport pathways and travel times. *Water Resour. Res.* 51, 7680–7701. <https://doi.org/10.1002/2014WR016689>.

Frey, K.E., McClelland, J.W., 2009. Impacts of permafrost degradation on arctic river biogeochemistry. *Hydrol. Process.* 23, 169–182. <https://doi.org/10.1029/2006JG000369>.

Frey, K.E., Siegel, D.L., Smith, L.C., 2007. Geochemistry of west Siberian streams and their potential response to permafrost degradation. *Water Resour. Res.* 43. <https://doi.org/10.1029/2006WR004902>.

Frey, K.E., Smith, L.C., 2005. Amplified carbon release from vast West Siberian peatlands by 2100. *Geophys. Res. Lett.* 32, L09401. <https://doi.org/10.1029/2004GL022025>.

Gat, J.R., 1996. Oxygen and hydrogen isotopes in the hydrological cycle. *Annu. Rev. Earth Planet Sci.* 24, 225–262.

Gibson, J., 2001. Forest-tundra water balance signals traced by isotopic enrichment in lakes. *J. Hydrol.* 251, 1–13.

Gibson, J.J., Birks, S.J., Edwards, T.W.D., 2008. Global prediction of δA and δH - $\delta^{18}\text{O}$ evaporation slopes for lakes and soil water accounting for seasonality. *Global Biogeochem. Cycles* 22 (2). <https://doi.org/10.1029/2007GB002997>.

Gibson, J.J., Yi, Y., Birks, S.J., 2016. Isotope-based partitioning of streamflow in the oil sands region, northern Alberta: Towards a monitoring strategy for assessing flow sources and water quality controls. *J. Hydrol.: Reg. Stud.* 5, 131–148. <https://doi.org/10.1016/j.ejrh.2015.12.062>.

Giesler, R., Lyon, S.W., Mörth, C., Karlsson, J., Karlsson, E., Jantze, E.J., et al., 2014. Catchment-scale dissolved carbon concentrations and export estimates across six subarctic streams in northern Sweden. *Biogeosciences* 11, 525–537.

Hayashi, M., Quinton, W.L., Pietroniro, A., Gibson, J.J., 2004. Hydrologic functions of wetlands in a discontinuous permafrost basin indicated by isotopic and chemical signatures. *J. Hydrol.* 296, 81–97.

IAEA/WMO, 2017. Global Network of Isotopes in Precipitation, the GNIP Database. Accessible at: <http://www.iaea.org/water>.

IPCC, 2014. Observations: Cryosphere, Climate Change 2013 – The Physical Science Basis: Working Group I Contribution to the Fifth Assessment Report of the Intergovernmental Panel on Climate Change. Cambridge University Press, Cambridge, pp. 317–382.

Jasechko, S., Kirchner, J.W., Welker, J.M., McDonnell, J.J., 2016. Substantial proportion of global streamflow less than three months old. *Nat. Geosci.* 9 (2), 126–129.

Jasechko, S., Wassenaar, L.I., Mayer, B., 2017. Isotopic evidence for widespread cold-season-biased groundwater recharge and young streamflow across central Canada. *Hydrol. Processes.* <https://doi.org/10.1002/hyp.11175>.

Karlsson, J.M., Lyon, S.W., Destouni, G., 2012. Thermokarst lake, hydrological flow and water balance indicators of permafrost change in Western Siberia. *J. Hydrol.* 464–465, 459–466. <https://doi.org/10.1016/j.jhydrol.2012.07.037>.

Kendall, C., McDonnell, J.J. (Eds.), 1998. *Isotope Tracers in Catchment Hydrology*. Elsevier.

Kirpotin, S.N., Berezin, A., Bazanov, V., Polishchuk, Y., Vorobiov, S., Mironycheva-Tokoreva, N., et al., 2009. Western Siberia wetlands as indicator and regulator of climate change on the global scale. *Int. J. Environ. Stud.* 66, 409–421.

Kuhry, P., Dorrepaal, E., Hugelius, G., Schuur, E., Tarnocai, C., 2010. Potential remobilization of belowground permafrost carbon under future global warming. *Permafrost Periglacial Processes* 21, 208–214.

- Kurita, N., Sugimoto, A., Fujii, Y., Fukazawa, T., Makarov, V.N., Watanabe, O., et al., 2005. Isotopic composition and origin of snow over Siberia. *J. Geophys. Res.* 110, D13102. <https://doi.org/10.1029/2004JD005053>.
- Kurita, N., Yoshida, N., Inoue, G., Chayanova, E.A., 2004. Modern isotope climatology of Russia: a first assessment. *J. Geophys. Res.* 109, D03102. <https://doi.org/10.1029/2003JD003404>.
- Lachniet, M.S., Lawson, D.E., Stephen, H., Sloat, A.R., Patterson, W.P., 2016. Isoscapes of $\delta^{18}\text{O}$ and $\delta^2\text{H}$ reveal climatic forcings on Alaska and Yukon precipitation. *Water Resour. Res.* 52, 6575–6586. <https://doi.org/10.1002/2016WR019436>.
- Lenderink, G., van Meijgaard, E., 2008. Increase in hourly precipitation extremes beyond expectations from temperature changes. *Nat. Geosci.* 1, 511–514.
- Lessels, J.S., Tetzlaff, D., Birkel, C., Dick, J., Soulsby, C., 2016. Water sources and mixing in riparian wetlands revealed by tracers and geospatial analysis. *Water Resour. Res.* 52, 456–470. <https://doi.org/10.1002/2015WR017519>.
- Lessels, J.S., Tetzlaff, D., Carey, S.K., Smith, P., Soulsby, C., 2015. A coupled hydrology–biogeochemistry model to simulate dissolved organic carbon exports from a permafrost-influenced catchment. *Hydrol. Process.* 29, 5383–5396. <https://doi.org/10.1002/hyp.10566>.
- Lindström, G., Bishop, K., Löfvenius, M.O., 2002. Soil frost and runoff at Svartberget, northern Sweden—measurements and model analysis. *Hydrol. Processes* 16, 3379–3392. <https://doi.org/10.1002/hyp.1106>.
- Lyon, S., Destouni, G., Giesler, R., Humborg, C., Mörth, C., Seibert, J., et al., 2009. Estimation of permafrost thawing rates in a sub-arctic catchment using recession flow analysis. *Hydrol. Earth Syst. Sci.* 13, 595–604.
- McClelland, J.W., Holmes, R.M., Peterson, B.J., Amon, R., Brabets, T., Cooper, L., et al., 2008. Development of a pan-Arctic database for river chemistry. *Eos, Trans. Am. Geophys. Union* 89, 217–218.
- McGuire, K.J., McDonnell, J.J., Weiler, M., Kendall, C., McGlynn, B.L., Welker, J.M., Seibert, J., 2005. The role of topography on catchment-scale water residence time. *Water Resour. Res.* 41. <https://doi.org/10.1029/2004WR003657>.
- McDonnell, J.J., Beven, K., 2014. Debates—The future of hydrological sciences: a (common) path forward? A call to action aimed at understanding velocities, celerities and residence time distributions of the headwater hydrograph. *Water Resour. Res.* 50, 5342–5350. <https://doi.org/10.1002/2013WR015141>.
- McNamara, J.P., Kane, D.L., Hinzman, L.D., 1997. Hydrograph separations in an Arctic watershed using mixing model and graphical techniques. *Water Resour. Res.* 33, 1707–1719.
- McVicar, T.R., Roderick, M.L., Donohue, R.J., Li, L.T., Van Niel, T.G., Thomas, A., Grieser, J., Jhajharia, D., Himri, Y., Mahowald, N.M., Mescherskaya, A.V., Kruger, A.C., Rehman, S., Dinpashov, Y., 2012. Global review and synthesis of trends in observed terrestrial near-surface wind speeds: Implications for evaporation. *J. Hydrol.* 416–417, 182–205. <https://doi.org/10.1016/j.jhydrol.2011.10.024>.
- Narancic, B., Wolfe, B.B., Pienitz, R., Meyer, H., Lamhonwah, D., 2017. Landscape-gradient assessment of thermokarst lake hydrology using water isotope tracers. *J. Hydrol.* 545, 327–338. <https://doi.org/10.1016/j.jhydrol.2016.11.028>.
- Novikov, S.M., Moskvina, Y.P., Trofimov, S.A., Usova, L.I., Batuev, V.I., Tumanovskaya, S.M., et al., 2009. Hydrology of bog territories of the permafrost zone of western Siberia. *BBM Publ. House, St. Petersburg* 535, pp. (in Russian).
- O'Donnell, J.A., Jorgenson, M.T., Harden, J.W., McGuire, A.D., Kanevskiy, M.Z., Wickland, K.P., 2012. The effects of permafrost thaw on soil hydrologic, thermal, and carbon dynamics in an Alaskan peatland. *Ecosystems* 15, 213–229. <https://doi.org/10.1007/s10021-011-9504-0>.
- Peralta-Tapia, A., Sponseller, R.A., Tetzlaff, D., Soulsby, C., Laudon, H., 2015. Connecting precipitation inputs and soil flow pathways to stream water in contrasting boreal catchments. *Hydrol. Process.* 29, 3546–3555. <https://doi.org/10.1002/hyp.10300>.
- Peterson, B.J., Holmes, R.M., McClelland, J.W., Vorosmarty, C.J., Lammers, R.B., Shiklomanov, A.I., et al., 2002. Increasing river discharge to the Arctic Ocean. *Science* 298, 2171–2173. <https://doi.org/10.1126/science.1077445>.
- Pokrovsky, O.S., Manasypov, R.M., Loiko, S.V., Krickov, I.A., Kopysov, S.G., Kolesnichenko, L.G., et al., 2016. Trace element transport in western Siberian rivers across a permafrost gradient. *Biogeosciences* 13, 1877.
- Pokrovsky, O., Manasypov, R., Loiko, S., Shirokova, L., Krickov, I., Pokrovsky, B., et al., 2015. Permafrost coverage, watershed area and season control of dissolved carbon and major elements in western Siberian rivers. *Biogeosciences* 12, 6301–6320. <https://doi.org/10.5194/bg-12-6301-2015>.
- Polishchuk, Y.M., Bogdanov, A.N., Polishchuk, V.Y., Manasypov, R.M., Shikorova, L.S., Kirpotin, S.N., et al., 2017. Size distribution, surface coverage, water, carbon, and metal storage of thermokarst lakes in the permafrost zone of the Western Siberia Lowland. *Water* 9. <https://doi.org/10.3390/w9030228>.
- Quinton, W.L., Roulet, N.T., 1998. Spring and summer runoff hydrology of a subarctic patterned wetland. *Arct. Alp. Res.* 30, 285–294.
- Quinton, W., Hayashi, M., Chasmer, L., 2011. Permafrost-thaw-induced land-cover change in the Canadian subarctic: implications for water resources. *Hydrol. Process.* 25, 152–158. <https://doi.org/10.1002/hyp.7894>.
- Quinton, W., Marsh, P., 1999. A conceptual framework for runoff generation in a permafrost environment. *Hydrol. Process.* 13, 2563–2581.
- Raudina, T.V., Loiko, S.V., Lim, A., Krickov, I.V., Shirokova, L.S., Istigechev, G.I., et al., 2017. Dissolved organic carbon, major and trace element in peat pore water of sporadic, discontinuous and continuous permafrost zone of Western Siberia. *Biogeosciences Discuss.* <https://doi.org/10.5194/bg-2017-24>.
- Romanovsky, V., Drozdov, D., Oberman, N., Malkova, G., Kholodov, A., Marchenko, S., et al., 2010. Thermal state of permafrost in Russia. *Permafrost Periglacial Processes* 21, 136–155.
- Serreze, M.C., Bromwich, D.H., Clark, M.P., Etringer, A.J., Zhang, T., Lammers, R., 2002. Large-scale hydro-climatology of the terrestrial Arctic drainage system. *J. Geophys. Res.* 107, 8160. <https://doi.org/10.1029/2001JD000919>.
- Shevchenko, V.P., Pokrovsky, O.S., Vorobyev, S.N., Krickov, I.V., Manasypov, R.M., Politova, N.V., et al., 2016. Impact of snow deposition on major and trace element concentrations and fluxes in surface waters of Western Siberian Lowland. *Hydrol. Earth Syst. Sci. Discuss.* <https://doi.org/10.5194/hess-2016-578>.
- Smith, A., Welch, C., Stadnyk, T., 2016. Assessment of a lumped coupled flow-isotope model in data scarce Boreal catchments. *Hydrol. Process.* <https://doi.org/10.1002/hyp.10835>.
- Smith, L.C., Alsdorf, D.E., 1998. Control on sediment and organic carbon delivery to the Arctic Ocean revealed with space-borne synthetic aperture radar: Ob'River, Siberia. *Geology* 26, 395–398.
- Smith, L.C., Beilman, D., Kremenetski, K.V., Sheng, Y., MacDonald, G.M., Lammers, R.B., et al., 2012. Influence of permafrost on water storage in West Siberian peatlands revealed from a new database of soil properties. *Permafrost Periglacial Processes* 23, 69–79. <https://doi.org/10.1002/ppp.735>.
- Smith, L.C., Pavelsky, T.M., MacDonald, G.M., Shiklomanov, A.I., Lammers, R.B., 2007a. Rising minimum daily flows in northern Eurasian rivers: a growing influence of groundwater in the high-latitude hydrologic cycle. *J. Geophys. Res.* 112. <https://doi.org/10.1029/2006JG000327>.
- Smith, L.C., Sheng, Y., MacDonald, G.M., 2007b. A first pan-Arctic assessment of the influence of glaciation, permafrost, topography and peatlands on northern hemisphere lake distribution. *Permafrost Periglacial Processes* 18, 201–208. <https://doi.org/10.1002/ppp.581>.
- Smith, L.C., Sheng, Y., MacDonald, G.M., Hinzman, L.D., 2005. Disappearing Arctic lakes. *Science* 308, doi:308/5727/1429 [pii].
- Song, C., Wang, G., Liu, G., Mao, T., Sun, X., Chen, X., 2017. Stable isotope variations of precipitation and streamflow reveal the young water fraction of a permafrost watershed. *Hydrol. Process.* 31, 935–947. <https://doi.org/10.1002/hyp.11077>.
- Soulsby, C., Birkel, C., Geris, J., Dick, J., Tunaley, C., Tetzlaff, D., 2015. Stream water age distributions controlled by storage dynamics and nonlinear hydrologic connectivity: Modeling with high-resolution isotope data. *Water Resour. Res.* 51, 7759–7776. <https://doi.org/10.1002/2015WR017888>.
- Streletskiy, D.A., Tananaev, N.I., Opel, T., Shiklomanov, N.I., Nyland, K.E., Streletskaya, I.D., et al., 2015. Permafrost hydrology in changing climatic conditions: seasonal variability of stable isotope composition in rivers in discontinuous permafrost. *Environ. Res. Lett.* 10, 095003. <https://doi.org/10.1088/1748-9326/10/9/095003>.
- Taylor, S., Feng, X., Williams, M., McNamara, J., 2002. How isotopic fractionation of snowmelt affects hydrograph separation. *Hydrol. Processes* 16 (18), 3683–3690.
- Tetzlaff, D., Birkel, C., Dick, J., Geris, J., Soulsby, C., 2014. Storage dynamics in hydrological units control hillslope connectivity, runoff generation, and the evolution of catchment transit time distributions. *Water Resour. Res.* 50, 969–985.
- Tetzlaff, D., Buttle, J., Carey, S.K., Huijgevoort, M.H., Laudon, H., McNamara, J.P., et al., 2015a. A preliminary assessment of water partitioning and ecohydrological coupling in northern headwaters using stable isotopes and conceptual runoff models. *Hydrol. Process.* 29, 5153–5173.
- Tetzlaff, D., Buttle, J., Carey, S.K., McGuire, K., Laudon, H., Soulsby, C., 2015b. Tracer-based assessment of flow paths, storage and runoff generation in northern catchments: a review. *Hydrol. Process.* 29, 3475–3490. <https://doi.org/10.1002/hyp.10412>.
- Tetzlaff, D., Soulsby, C., Buttle, J., Capell, R., Carey, S.K., Laudon, H., et al., 2013. Catchments on the cusp? Structural and functional change in northern ecohydrology. *Hydrol. Process.* 27, 766–774. <https://doi.org/10.1002/hyp.9700>.
- Throckmorton, H.M., Newman, B.D., Heikoop, J.M., Perkins, G.B., Feng, X., Graham, D.E., et al., 2016. Active layer hydrology in an arctic tundra ecosystem: quantifying water sources and cycling using water stable isotopes. *Hydrol. Process.* 30, 4972–4986. <https://doi.org/10.1002/hyp.10883>.
- Ulmishek, G.F., 2003. Petroleum geology and resources of the West Siberian Basin, Russia, US Department of the Interior, US Geological Survey.
- Vasil'chuk, Y.K., Shevchenko, V., Lisitzin, A., Budantseva, N., Vorobiov, S., Kirpotin, S., et al., 2016. Oxygen isotope and deuterium composition of snow cover on the profile of Western Siberia from Tomsk to the Gulf of Ob. *Dokl. Earth Sc.* 471, 1284–1287. <https://doi.org/10.1134/S1028334X1612014X>.
- Walvoord, M.A., Kurylyk, B.L., 2016. Hydrologic impacts of thawing permafrost – a review. *Vadose Zone J.* 15. <https://doi.org/10.2136/vzj2016.01.0010>.
- Welp, L., Randerson, J., Finlay, J., Davydov, S., Zimova, G., Davydova, A., et al., 2005. A high-resolution time series of oxygen isotopes from the Kolyma River: implications for the seasonal dynamics of discharge and basin-scale water use. *Geophys. Res. Lett.* 32, L14401. <https://doi.org/10.1029/2005GL022857>.
- White, D., Hinzman, L., Alessa, L., Cassano, J., Chambers, M., Falkner, K., et al., 2007. The arctic freshwater system: changes and impacts. *J. Geophys. Res. Biogeosci.* 112. <https://doi.org/10.1029/2006JG000353>.
- Wild, M., 2009. Global dimming and brightening: a review. *J. Geophys. Res. Atmos.* 114. <https://doi.org/10.1029/2008JD011470>.
- Willett, K.M., Jones, P.D., Gillett, N.P., Thorne, P.W., 2008. Recent changes in surface humidity: development of the HadCRUH dataset. *J. Clim.* 21, 5364–5383.
- Woo, M., 1986. Permafrost hydrology in north America. *Atmos. Ocean* 24, 201–234.
- Woo, M., Kane, D.L., Carey, S.K., Yang, D., 2008. Progress in permafrost hydrology in the new millennium. *Permafrost Periglacial Processes* 19, 237–254. <https://doi.org/10.1002/ppp.613>.

- Yang, D., Ye, B., Shiklomanov, A., 2004. Discharge characteristics and changes over the Ob River watershed in Siberia. *J. Hydrometeorol.* 5, 595–610.
- Yang, Y., Wu, Q., Hou, Y., Zhang, Z., Zhan, J., Gao, S., Jin, H., 2017. Unraveling of permafrost hydrological variabilities on Central Qinghai-Tibet Plateau using stable isotopic technique. *Sci. Total Environ.* 605–606, 199–210. <https://doi.org/10.1016/j.scitotenv.2017.06.213>.
- Ye, H., Ladochy, S., Yang, D., Zhang, T., Zhang, X., Ellison, M., 2004. The impact of climatic conditions on seasonal river discharges in Siberia. *J. Hydrometeorol.* 5, 286–295.
- Yi, Y., Gibson, J.J., Hélie, J.F., Dick, T.A., 2010. Synoptic and time-series stable isotope surveys of the Mackenzie River from Great Slave Lake to the Arctic Ocean, 2003 to 2006. *J. Hydrol.* 383, 223–232. <https://doi.org/10.1016/j.jhydrol.2009.12.038>.
- Yi, Y., Gibson, J., Cooper, L.W., Hélie, J., Birks, S., McClelland, J.W., et al., 2012. Isotopic signals (^{18}O , 2H , 3H) of six major rivers draining the pan-Arctic watershed. *Global Biogeochem. Cycles* 26. <https://doi.org/10.1029/2011GB004159>.
- Zakharova, E., Kouraev, A., Biancamaria, S., Kolmakova, M., Mognard, N., Zemtsov, V., et al., 2011. Snow cover and spring flood flow in the Northern Part of Western Siberia (the Poluy, Nadym, Pur, and Taz Rivers). *J. Hydrometeorol.* 12, 1498–1511.
- Zakharova, E., Kouraev, A., Kolmakova, M., Mognard, N., Zemtsov, V., Kirpotin, S., 2009. The modern hydrological regime of the northern part of Western Siberia from in situ and satellite observations. *Int. J. Environ. Stud.* 66, 447–463.
- Zakharova, E.A., Kouraev, A.V., Rémy, F., Zemtsov, V.A., Kirpotin, S.N., 2014. Seasonal variability of the Western Siberia wetlands from satellite radar altimetry. *J. Hydrol.* 512, 366–378. <https://doi.org/10.1016/j.jhydrol.2014.03.002>.
- Zhou, J., Wu, J., Liu, S., Zeng, G., Qin, J., Wang, X., Zhao, Q., 2015. Hydrograph separation in the headwaters of the Shule River basin: combining water chemistry and stable isotopes. *Adv. Meteorol.* 830308. <https://doi.org/10.1155/2015/830306>.